Arch. Pharm. Res.
DOI 10.1007/s12272-017-0977-z

Online ISSN 1976-3786
Print ISSN 0253-6269

Archives of Pharmacal Research
www.springer.com/12272

RESEARCH ARTICLE

Design, synthesis and evaluation of alkylphosphocholine-gefitinib conjugates as multitarget anticancer agents

Md. Maqusood Alam[1] · Ahmed H. E. Hassan[2,3] · Yeong Ho Kwon[1] · Hyo Jong Lee[1] · Nam Yong Kim[1] · Kyung Hoon Min[4] · Sang-Yoon Lee[5] · Dong-Hyun Kim[1] · Yong Sup Lee[1,3]

Received: 20 June 2017 / Accepted: 19 October 2017

Abstract The evolving resistance to the currently used chemotherapeutic agents requires continuous efforts to develop new anticancer agents overcoming resistance and with lower side effects. Polypharmacology via designing a single molecule intercepting multiple signaling pathways is more effective than targeting a single one. Several alkylphosphocholines show anticancer activity via inhibition of Akt phosphorylation. On the other hand, several molecules having quinazoline scaffold elicit anticancer activity through inhibition of epidermal growth factor receptor (EGFR) tyrosine kinases. We report our efforts to develop alkylphosphocholines-gefitinib conjugates as multitarget anticancer agents. The antiproliferative activities of the newly synthesized compounds were evaluated against cell lines representing lung, breast, liver and skin cancers. In addition, the capability of the newly synthesized compounds to inhibit Akt phosphorylation and EGFR tyrosine kinases were determined. The results emphasized the influence of the linkers' length on the elicited bioactivity. The long chain linkers possessing conjugates were more active regarding both of the elicited antiproliferative effect and inhibition of Akt phosphorylation, while maintained the ability to inhibit EGFR tyrosine kinases. Their cytotoxic activities were superior or comparable to erlotinib and miltefosine.

Keywords Alkylphosphocholines · Gefitinib · Akt phosphorylation inhibitors · EGFR tyrosine kinase inhibitors · Antiproliferartive agents

✉ Yong Sup Lee
kyslee@khu.ac.kr

[1] Department of Life and Nanopharmaceutical Sciences, Kyung Hee University, Seoul 02447, Republic of Korea

[2] Department of Medicinal Chemistry, Faculty of Pharmacy, Mansoura University, Mansoura 35516, Egypt

[3] Medicinal Chemistry Laboratory, Department of Pharmacy, College of Pharmacy, Kyung Hee University, Seoul 02447, Republic of Korea

[4] Department of Pharmacy, College of Pharmacy, Chung-Ang University, Seoul 06974, Republic of Korea

[5] Neuroscience Research Institute, Gachon University, Incheon 20565, Republic of Korea

Introduction

Cancer cells differs from normal cells in uptake and metabolism of lipids (Beloribi-Djefaflia et al. 2016). Increased lipids uptake by cancer cells enabled development of visualizing agents for cancer cells via alkylphosphocholine-based hybrid molecules for delivering imaging agents into cancer cells (Weichert et al. 2014). CLR1404 (**1a**, Fig. 1) is a radiolabeled molecule that has been proposed for PET-imaging of tumors. Also, CLR1502 (**1b**, Fig. 1) which incorporates the infrared dye IR-775 might be suitable for intraoperative surgical detection of tumor's margin. In fact, some alkylphosphocholines (APCs) elicit antitumor activities by themselves (Pachioni Jde et al. 2013; Faustino 2014; Kostadinova et al. 2015; Murray et al. 2015). They may integrate into tumor cell's membrane changing its properties, trafficking and signaling. In addition, they may interfere with lipids metabolism and lipids-dependent signaling cascades (Danker et al. 2010; van Blitterswijk and Verheij 2013; Faustino 2014). Miltefosine **2** (miltex®) is a prominent members of this class of compounds. However, gastrointestinal toxicity restricts its use to topical treatment of cutaneous metastasis of breast cancer (Clive et al. 1999). Several studies indicate that

Published online: 01 November 2017

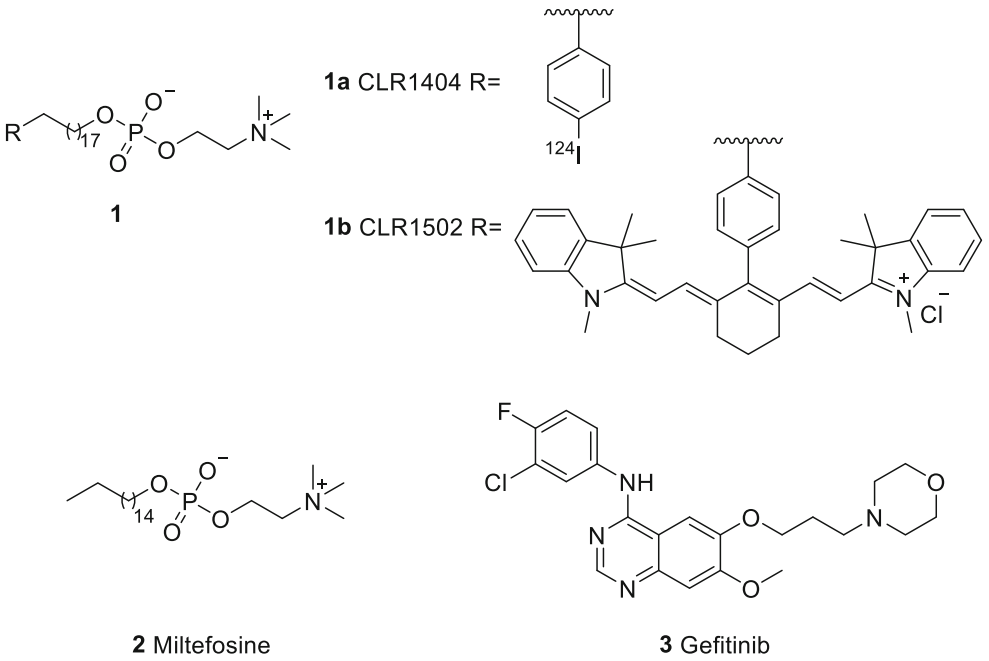

Fig. 1 Structures of reported alkylphosphocholines and gefitinib

APCs such as miltefosine **2** can form highly stable complexes with the cholesterol-enriched rigid domains within the cell membrane known as lipid rafts (Gomez-Serranillos et al. 2004; Malta de Sá et al. 2015). Lipid rafts modulate multiple signaling pathways (Simons and Toomre 2000; Pike 2003; Fielding and Fielding 2004). PI3K/Akt signaling pathway is one of these pathways impacted by lipid rafts (Reis-Sobreiro et al. 2013). Cholesterol synthesis inhibition or sequestration from lipid rafts down-regulates Akt signaling (Zhuang et al. 2005; Fedida-Metula et al. 2008; Calay et al. 2010). The anticancer properties of APC derivatives mediated via modulation of PI3K/Akt pathway are known (Alam et al. 2012, 2013).

Gefitinib (**3**, Iressa) is a FDA approved kinase inhibitor for the treatment of EGFR-mutated lung cancer in which EGFR mutations abolish the activity of the wild EGFR inhibitors such as erlotinib (Kazandjian et al. 2016). Unfortunately, gefitinib resistance arise because of activation of PI3K/AKT pathway, at least in part (Li et al. 2013). It is known that PI3K/AKT pathway communicates synergistically with the EGFR signaling (Block et al. 2012). A combination of gefitinib and RAD001, an inhibitor of PI3K/AKT pathway, was found to elicit synergistic inhibition of cancer cell lines (Dragowska et al. 2011). Importantly, the PI3K/AKT pathway inhibitor LY294002 was reported to restore the sensitivity to gefitinib in resistant cell lines (Li et al. 2013).

Polypharmacology via design of a single molecule intercepting multiple signaling pathways could be more effective than the simple combination therapy. A single bifunctional molecule inhibiting both of PI3K/AKT and EGFR pathways might be a useful strategy for developing novel anticancer agents. Investigation of the reported crystals of gefitinib-EGFR complex (PDB codes 3UG2 and 4WKQ) shows that the aromatic rings of the quinazoline core of gefitinib (**3**) interact with the hydrophobic pocket of EGFR while the aliphatic alkoxy substituents extends outside of the binding site. Accordingly, modification of the alkoxy substituents is anticipated to maintain the affinity of the molecule to the binding pocket of EGFR. On the other hand, analogues of miltefosine **2** such as CLR1404 and CLR1502 which have moieties conjugated to the terminal end of the alkyl chain maintained selectivity to cancerous cells. Based on this, analogues of miltefosine (**2**) conjugated with the core of gefitinib via hydroxyalkanoic acids linkers might result in useful multitarget anticancer agent with increased the efficacy (Fig. 2). In the designed conjugated molecules, the impact of the length of the alkyl chain of the APCs and moiety, as well as, the linker would be investigated. Herein, we would like to report our results.

Materials and methods

Chemistry

General

All solvents were purified and used on scrupulously dry condition. NMR spectra of all compounds were recorded on Bruker AC-400 spectrometer (400 MHz for ^{1}H and 100 MHz for ^{13}C). Chemical shifts (δ) are reported in ppm,

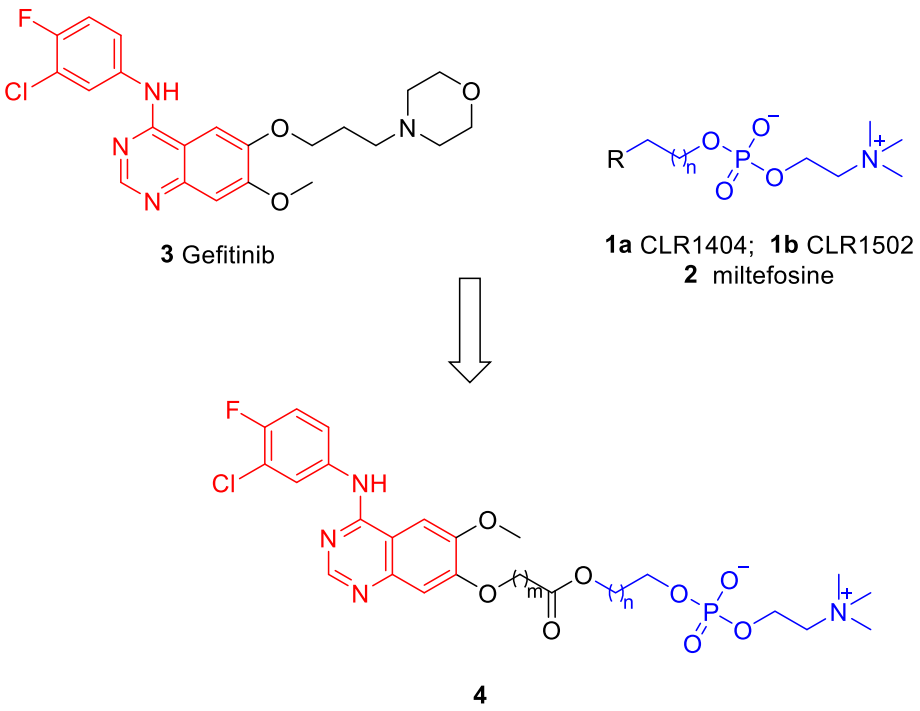

Fig. 2 Design of alkylphosphocholine-gefitinib conjugates

downfield from internal TMS standard. High resolution mass spectra (HRMS) were recorded on Jeol AccuTOF (JMS-T100TD) equipped with a DART (direct analysis in real time) ion source from ionsense, Tokyo, Japan in the positive modes. Analytical thin layer chromatography (TLC) was carried out using precoated silica gel (E. Merck Kiesegel 60F254, layer thickness 0.25 mm), and chromatography was performed using Merck Kiesegel 60 Art 9385 (230–400 mesh).

7-(Benzyloxy)-N-(3-chloro-4-flurophenyl)-6-methoxyquinazoline-4-amine (6)

A mixture of 7-(benzyloxy)-4-chloro-6-methoxyquinazoline **5** (2.0 g, 6.6 mmol) and 3-chloro-4-fluoroaniline (1.1 g, 7.9 mmol) in *i*-PrOH (20.0 mL) was refluxed for 4 h. Upon cooling to rt, the precipitated crystals were filtered, washed with *i*-PrOH, ether and dried to give compound **6**. Yield 96%. ^{1}H-NMR (400 MHz, DMSO-d_6) δ: 4.02 (s, 3H), 5.34 (s, 2H), 7.76-7.37 (m, 8H), 8.03 (d, 1H, $J = 6.7$ Hz), 8.31 (s, 1H), 8.84 (s, 1H).

4-(3-Chloro-4-flurophenylamino)-6-methoxyquinazolin-7-ol (7)

A mixture of compound **6** (2.6 g, 6.3 mmol) and trifluoroacetic acid (20.0 mL) was refluxed for 1 h, cooled to rt, filtered, dissolved in methanol (10.0 mL), and then the pH was adjusted to 9–10 with ammonium hydroxide (25% aq. solution). Concentration in vacuo, filtration and washing with water followed by ether yielded the titled compound **7**. Yield 98%. ^{1}H-NMR (400 MHz, DMSO-d_6) δ: 4.00 (s, 3H), 7.28-7.04 (M, 2H), 7.48 (s, 1H), 7.84 (m, 1H), 8.56 (s, 1H), 8.80 (s, 1H).

General procedure for the synthesis of ethyl 7-(4-(3-chloro-4-fluorophenylamino)-6-methoxyquinazolin-7-yloxy)alkanoates (8)

A mixture of compound **7** (1.0 mmol), ethyl bromoalkanoate (1.2 mmol) and potassium carbonate (3.0 mmol) in DMF was stirred at 60 °C for 4 h. The mixture was cool to rt and filtered. The filtrate was concentrated in vacuo. The residue was dissolved in dichloromethane and washed with brine, dried over magnesium sulfate and concentrated to afford derivatives **8**.

Ethyl 7-(4-(3-chloro-4-fluorophenylamino)-6-methoxyquinazolin-7-yloxy)heptanoate (8a)

Yield 89%. ^{1}H-NMR (400 MHz, DMSO-d_6) δ: 1.18 (t, 3H, $J = 7.2$ Hz), 1.57-1.32 (m, 6H), 1.82-1.74 (m, 2H), 2.32 (t, 3H, $J = 7.2$ Hz), 4.02-4.08 (m, 5H), 4.16 (t, 2H, $J = 6.2$ Hz), 7.35 (s, 1H), 7.53 (t, 1H, $J = 9.0$ Hz), 7.79-7.76 (m, 1H), 8.04 (d, 1H, $J = 6.7$ Hz), 8.38 (s, 1H), 8.85 (s, 1H), 11.6 (s, 1H).

Ethyl 2-(4-(3-chloro-4-fluorophenylamino)-6-methoxyquinazolin-7-yloxy)acetate (8b)

Yield 71%. ^{1}H-NMR (400 MHz, DMSO-d_6) δ: 1.18 (t, 3H, $J = 7.2$ Hz), 4.13-3.84 (m, 7H), 6.91 (s, 1H), 7.38 (t, 1H, $J = 9.1$ Hz), 7.97-7.93 (m, 2H), 8.27 (d, 1H, $J = 6.7$ Hz), 8.34 (s, 1H), 9.78 (s, 1H).

General procedure for the synthesis of 7-(4-(3-chloro-4-fluorophenylamino)-6-methoxyquinazolin-7-yloxy)alkanoic acids (9)

Lithium hydroxide monohydrate (3.0 mmol) was added to a solution of ethyl 7-(4-(3-chloro-4-fluorophenylamino)-6-methoxyquinazolin-7-yloxy)alkanoates **8** (1.0 mmol) in THF (18.0 mL) and distilled water (6.0 mL). The solution was stirred for 24 h. The reaction mixture cooled in an ice bath was acidified to pH 2 with HCl (1 N aq. solution). The solids were filtered, washed with distilled water and dried to yield the titled derivatives **9**.

7-(4-(3-Chloro-4-fluorophenylamino)-6-methoxyquinazolin-7-yloxy)heptanoic acid (9a)

Yield 91%. ^{1}H-NMR (400 MHz, DMSO-d_6) δ: 1.81-1.44 (m, 8H), 2.20-2.02 (m, 2H), 3.96 (s, 3H), 4.14-4.11 (t, 2H, $J = 6.4$ Hz), 7.18 (s, 1H), 7.44 (t, 1H, $J = 9.1$ Hz), 7.82 (s, 1H), 8.14 (m, 1H), 8.48 (s, 1H) 9.58 (s, 1H).

2-(4-(3-Chloro-4-fluorophenylamino)-6-methoxyquinazolin-7-yloxy)acetic acid (9b)

Yield 90%. ^{1}H-NMR (400 MHz, DMSO-d_6) δ: 4.00 (s, 3H), 4.24 (s, 2H), 7.05 (s, 1H), 7.26 (t, 1H, $J = 8.9$ Hz), 7.57-7.48 (m, 1H), 7.86-7.82(m, 2H), 8.56 (s, 1H).

General procedure for the synthesis of benzyloxyalkyl 2-(trimethylammonio)ethyl phosphates (13)

2-Chloro-1,3,2-dioxaphospholane 2-oxide (2.0 mmol) was added to a stirred solution of compound **12** (1.0 mmol) in benzene (5.0 mL) containing triethylamine (2.0 mmol) at 0 °C. After warming up slowly to rt, the reaction mixture was stirred for 4 h. The precipitated triethylamine hydrochloride was filtered and washed with benzene. The combined filtrate and washings was concentrated, diluted with CH_3CN (10.0 mL) and transferred into pressure tube. After cooling to −78 °C, trimethylamine was added (ca. 1.5 mL). The tube was closed, heated at 65 °C for 18 h, cooled back to rt and evaporated. The residual solid was purified by column chromatography on silica gel, first eluting with $CHCl_3$-MeOH (9:1) for separation of nonpolar product, and then with $CHCl_3$-MeOH-H_2O (65:20:4). The obtained semi-solids were precipitated from chloroformic solutions with *n*-pentane to afford **13**.

9-(Benzyloxy)nonyl 2-(trimethylammonio)ethyl phosphate (13a)

Yield 88%. ^{1}H-NMR (400 MHz, methanol-d_4) δ: 1.46-1.32 (m, 10H), 1.83-1.57 (m, 4H), 3.23 (s, 9H), 3.49 (t, 1H, $J = 6.4$ Hz), 3.65-3.63 (m, 2H), 3.72 (t, 1H, $J = 5.1$ Hz), 3.88 (q, 2H, $J = 6.8$ Hz), 3.98-3.94 (m, 2H), 4.34-4.24 (m, 2H), 7.37-7.26 (m, 3H), 7.51-7.46 (m, 1H), 8.04-8.01 (m, 1H).

10-(Benzyloxy)decyl 2-(trimethylammonio)ethyl phosphate (13b)

Yield 83%. ^{1}H-NMR (400 MHz, methanol-d_4) δ: 1.46-1.31 (m, 12H), 1.83-1.57 (m, 4H), 3.23 (s, 9H), 3.49 (t, 1H, $J = 6.4$ Hz), 3.65-3.64 (m, 2H), 3.72 (t, 1H, $J = 5.1$ Hz), 3.88 (q, 2H, $J = 6.8$ Hz), 3.98-3.94 (m, 2H), 4.34-4.24 (m, 2H), 7.37-7.26 (m, 3H), 7.51-7.45 (m, 1H), 8.04-8.01 (m, 1H).

12-(Benzyloxy)dodecyl 2-(trimethylammonio)ethyl phosphate (13c)

Yield 53%. ^{1}H-NMR (400 MHz, methanol-d_4) δ: 1.46-1.33 (m, 16H), 1.83-1.58 (m, 4H), 3.23 (s, 9H), 3.49 (t, 1H, $J = 6.4$ Hz), 3.65-3.63 (m, 2H), 3.72 (t, 1H, $J = 5.1$ Hz), 3.88 (q, 2H, $J = 6.8$ Hz), 3.98-3.95 (m, 2H), 4.34-4.24 (m, 2H), 7.37-7.28 (m, 3H), 7.51-7.46 (m, 1H), 8.04-8.01 (m, 1H).

General procedure for the synthesis of hydroxyalkyl 2-(trimethylammonio)ethyl phosphates (14)

To a solution of compound **13** (1.0 mmol) in methanol (10.0 mL) 10% Pd/C was added (catalytic amount). The reaction was stirred under hydrogen for 4 h at rt. The mixture was filtered and evaporated under vacuum to afford **14**.

9-Hydroxynonyl 2-(trimethylammonio)ethyl phosphate (14a)

Yield 96%. ^{1}H-NMR (400 MHz, methanol-d_4) δ: 1.54-1.29 (m, 12H), 1.65-1.60 (m, 2H), 3.22 (s, 9H), 3.64-3.51 (m, 4H), 3.92-3.85 (m, 2H), 4.32-4.18 (m, 2H).

10-Hydroxydecyl 2-(trimethylammonio)ethyl phosphate (14b)

Yield 92%. ^{1}H-NMR (400 MHz, methanol-d_4) δ: 1.40-1.22 (m, 12H), 1.54-1.50 (m, 2H), 1.66-1.61 (m, 2H), 3.23 (s, 9H), 3.54 (t, 2H, J = 5.3 Hz), 3.66-3.62 (m, 2H), 3.90-3.86 (m, 2H), 4.27 (m, 2H).

12-Hydroxydodecyl 2-(trimethylammonio)ethyl phosphate (14c)

Yield 93%. ^{1}H-NMR (400 MHz, methanol-d_4) δ: 1.40-1.22 (m, 16H), 1.54-1.50 (m, 2H), 1.66-1.61 (m, 2H), 3.23 (s, 9H), 3.54 (t, 2H, J = 5.3 Hz), 3.66-3.62 (m, 2H), 3.90-3.86 (m, 2H), 4.27 (m, 2H).

General procedure for the synthesis of 9-(7-(4-(3-chloro-4-fluorophenylamino)-6-methoxyquinazolin-7-yloxy)alkanoyloxy) alky 2-(trimethylammonio)ethyl phosphates (4)

Hydroxyalkyl 2-(trimethylammonio)ethyl phosphate **14** (1.0 mmol) was dissolved in anhydrous $CHCl_3$ (20.0 mL) and DMF (2.0 mL) and the mixture was heated to reflux under an atmosphere of N_2. DMAP (3.0 mmol), 7-(4-(3-chloro-4-fluorophenylamino)-6-methoxyquinazolin-7-yloxy) alkanoic acid **11** (3.0 mmol) and DCC (3.0 mmol) were added. The reaction mixture was refluxed for 24 h. The reaction mixture was cooled to rt. The residual semisolid was purified by column chromatography on silica gel, first eluting with $CHCl_3$-MeOH (9:1) for separation of nonpolar product, and then with $CHCl_3$-MeOH-H_2O (65:20:4).

9-(7-(4-(3-Chloro-4-fluorophenylamino)-6-methoxyquinazolin-7-yloxy)heptanoyloxy) nonyl 2-(trimethylammonio)ethyl phosphate (4aa)

Yield 50%. ^{1}H-NMR (400 MHz, methanol-d_4) δ: 1.38-1.19 (m, 12H), 1.81-1.42 (m, 10H), 2.31 (t, 2H, J = 7.2 Hz), 3.11 (s, 9H), 3.64-3.50 (m, 2H), 3.85 (q, 2H, J = 6.5 Hz), 3.93 (s, 3H), 4.08 (t, 2H, J = 6.5 Hz), 4.15 (t, 2H, J = 6.1 Hz), 4.21-4.05 (m, 4H), 7.02 (s, 1H), 7.16 (t, 1H, J = 7.9 Hz), 7.62-7.56 (m, 2H), 7.91 (d, 1H, J = 6.7 Hz), 8.33 (s, 1H). ^{13}C-NMR (100 MHz, methanol-d_4) δ: 175.6, 158.3, 156.2, 153.7, 151.5, 147.6, 137.6, 130.4, 125.8, 123.9, 121.4, 117.5, 110.3, 107.7, 102.4, 70.0, 67.5, 66.9, 65.5, 60.3, 56.9, 54.7, 54.7, 54.7, 35.1, 31.9, 31.8, 30.6, 30.4, 30.3, 29.8, 29.8, 27.1, 26.9, 26.8, 26.0. HRMS *m/z* 755.3345 (calcd for $C_{36}H_{54}ClFN_4O_8P$ $[M+H]^+$ 755.3346).

10-(7-(4-(3-Chloro-4-fluorophenylamino)-6-methoxyquinazolin-7-yloxy)heptanoyloxy) decyl 2-(trimethylammonio)ethyl phosphate (4ab)

Yield 88%. ^{1}H-NMR (400 MHz, methanol-d_4) δ:1.47-1.27 (m, 14H), 1.68-1.51 (m, 8H), 1.91-1.85 (m, 2H), 2.31 (t, 2H, J = 7.2 Hz), 3.20 (s, 9H), 3.62-3.59 (m, 2H), 3.83 (q, 2H, J = 6.5 Hz), 4.02 (s, 3H), 4.08 (t, 2H, J = 6.5 Hz), 4.25-4.10 (m, 4H), 7.10 (s, 1H), 7.24 (t, 1H, J = 7.9 Hz), 7.70-7.66 (m, 2H), 8.00 (d, 1H, J = 6.7 Hz), 8.42 (s, 1H). ^{13}C-NMR (100 MHz, methanol-d_4) δ: 174.2, 156.9, 155.4, 154.7, 152.3, 150.1, 146.3, 136.2, 124.3, 122.3, 120.0, 116.0, 106.3, 101.0, 102.4, 70.0, 66.0, 65.4, 64.1, 58.9, 55.5, 53.3, 53.3, 53.2, 33.6, 30.5, 29.3, 29.0, 22.2, 29.0, 28.4, 28.4, 28.4, 25.7, 25.5, 25.4, 24.6. HRMS *m/z* 769.3506 (calcd for $C_{37}H_{56}ClFN_4O_8P$ $[M+H]^+$ 769.3503).

12-(7-(4-(3-Chloro-4-fluorophenylamino)-6-methoxyquinazolin-7-yloxy)heptanoyloxy) dodecyl 2-(trimethylammonio)ethyl phosphate (4ac)

Yield 63%. ^{1}H-NMR (400 MHz, methanol-d_4) δ: 1.47-1.25 (m, 18H), 1.68-1.51 (m, 8H), 1.91-1.85 (m, 2H), 2.31 (t, 2H, J = 7.2 Hz), 3.20 (s, 9H), 3.62-3.59 (m, 2H), 3.83 (q, 2H, J = 6.5 Hz), 4.02 (s, 3H), 4.08 (t, 2H, J = 6.5 Hz), 4.15 (t, 2H, J = 6.1 Hz), 4.27-4.20 (m, 2H), 7.13 (s, 1H), 7.25 (t, 1H, J = 7.9 Hz), 7.70-7.66 (m, 2H), 8.00 (d, 1H, J = 6.7 Hz), 8.42 (s, 1H). ^{13}C-NMR (100 MHz, methanol-d_4) δ: 174.4, 157.1, 155.6, 154.9, 153.7, 152.5, 150.3, 146.4, 136.5, 124.5, 122.5, 120.0, 116.3, 109.1, 106.5, 101.2, 68.8, 66.3, 65.8, 64.4, 59.1, 59.0, 53.5, 53.5, 53.5, 33.9, 30.7, 29.8, 29.6, 29.5, 29.5, 29.3, 29.2, 28.7, 28.6, 28.6, 28.6, 28.6, 25.9. HRMS *m/z* 797.3824 (calcd for $C_{39}H_{60}ClFN_4O_8P$ $[M+H]^+$ 797.3816).

9-(2-(4-(3-Chloro-4-fluorophenylamino)-6-methoxyquinazolin-7-yloxy)acetoxy)nonyl 2-(trimethylammonio)ethyl phosphate (4ba)

Yield 80%. ^{1}H-NMR (400 MHz, methanol-d_4) δ: 1.58-1.05 (m, 14H), 3.11 (s, 9H), 3.56-3.49 (m, 2H), 3.77 (q, 2H, J = 6.5 Hz), 3.91(s, 3H), 4.18-4.11 (m, 4H), 4.83 (s, 2H), 6.84 (s, 1H), 7.72-7.18 (m, 2H), 7.43-7.41 (m, 1H), 7.80 (s, 1H), 8.85 (s, 1H). ^{13}C-NMR (100 MHz, methanol-d_4) δ: 168.8, 157.1, 155.7, 153.8, 152.7, 150.1, 146.1, 133.0, 129.2, 128.4, 122.6, 120.2, 116.3, 107.5, 101.9, 66.1, 65.5, 65.3, 65.2, 58.9, 55.7, 53.3, 53.3, 53.2, 30.5, 30.4, 29.2, 29.2, 29.0, 28.3, 25.6. HRMS *m/z* 685.2609 (calcd for $C_{31}H_{44}ClFN_4O_8P$ $[M+H]^+$ 685.2564).

10-(2-(4-(3-Chloro-4-fluorophenylamino)-6-methoxyquinazolin-7-yloxy)acetoxy)decyl 2-(trimethylammonio)ethyl phosphate (4bb)

Yield 58%. ^{1}H-NMR (400 MHz, methanol-d_4) δ: 1.35-1.17 (m, 12H), 1.63-1.54 (m, 4H), 3.12 (s, 9H), 3.63-3.60 (m, 2H), 3.83 (q, 2H, $J = 6.5$ Hz), 4.05 (s, 3H), 4.26-4.19 (m, 4H), 4.93 (s, 2H), 7.06 (s, 1H), 7.26 (t, 1H, $J = 8.9$ Hz), 7.72-7.68 (m, 2H), 7.78 (s, 1H), 8.43 (s, 1H). ^{13}C-NMR (100 MHz, methanol-d_4) δ: 168.6, 156.9, 155.7, 153.4, 153.3, 152.5, 149.9, 145.9, 136.1, 124.3, 122.4, 120.0, 116.1, 109.7, 107.3, 101.7, 66.1, 65.5, 65.3, 65.2, 58.9, 55.7, 53.3, 53.3, 53.2, 30.5, 30.4, 29.2, 29.0, 28.9, 28.3, 25.5. HRMS *m/z* 699.2715 (calcd for $C_{32}H_{46}ClFN_4O_8P$ $[M+H]^+$ 699.2720).

12-(2-(4-(3-Chloro-4-fluorophenylamino)-6-methoxyquinazolin-7-yloxy)acetoxy)dodecyl 2-(trimethylammonio)ethyl phosphate (4bc)

Yield 73%. ^{1}H-NMR (400 MHz, methanol-d_4) δ: 1.37-1.14 (m, 16H), 1.63-1.56 (m, 4H), 3.21 (s, 9H), 3.63-3.60 (m, 2H), 3.85 (q, 2H, $J = 6.6$ Hz), 4.05 (s, 3H), 4.26-4.19 (m, 4H), 4.94 (s, 1H), 7.06 (s, 1H), 7.26 (t, 1H, $J = 8.9$ Hz), 7.72-7.68 (m, 2H), 7.78 (s, 1H), 8.03 (d, 1H, $J = 6.6$ Hz), 8.44 (s, 1H). ^{13}C-NMR (100 MHz, methanol-d_4) δ: 170.0, 158.4, 155.7, 154.8, 153.9, 151.3, 147.3, 137.6, 125.7, 123.8, 121.4, 117.5, 117.3 116.2, 108.7, 103.1, 67.5, 67.0, 66.7, 66.6, 60.3, 57.1, 54.7, 54.7, 54.7, 31.9, 31.9, 30.7, 30.7, 30.4, 30.3, 29.7, 27.0, 26.9. HRMS *m/z* 727.3068 (calcd for $C_{34}H_{50}ClFN_4O_8P$ $[M+H]^+$ 727.3033).

Biological evaluation

Cell viability MTT assay

A549, MCF-7, HepG2 and A431 cell lines were purchased from Korean cell line bank (KCLB). Cell lines were grown under humidified atmosphere containing 5% CO_2 at 37 °C with Dulbecco's Modified Eagle's Medium (DMEM) and 10% (v/v) heat inactivated fetal bovine serum (FBS). Cells were placed into 96-well plates at a density of 5×10^3 cells/mL per well, treated with compounds to be tested. After incubation for 2 days under humidified atmosphere containing 5% CO_2 at 37 °C, the cells were harvested, treated with 10 μL of Dye Solution (Cell Titer 96, Promega, Madison, WI) and incubated at 37 °C under 5% CO_2 for 4 h. Then, 100 μL of solubilization solution/stop mix was added and the plates were left to stand for overnight. The absorbance at 570 nm was measured with a microplate reader (VersaMax,Molecular Devices, and Sunnyvale, CA, USA) and the data are presented as % inhibitions of the cell growth.

Akt phosphorylation inhibitory activity assay

A549 human lung cancer cell line was grown to 70% confluency and serum starved for 18 h. Cells were incubated for 2 h with 20 μM concentrations of each compound or miltefosine after which Akt phosphorylation was stimulated by adding insulin at 10 μg/mL and incubated for further 30 min. As a negative control, insulin was not added and positive control insulin was added for 30 min. For the control of an active Akt pathway, the Akt phosphorylation inhibitors, miltefosine, was added for 2 h prior to addition of insulin and showed in all cases lack of Akt phosphorylation. After 30 min stimulation with insulin, the cells were washed in ice-cold PBS and lysed using RIPA lysis buffer (Sigma-Aldrich, MO, USA) before performing the ELISA-based phosphor-Akt assay kit (R&D systems, MN, USA) according to the manufacturer's protocol. Data are presented as the means of three independent experiments.

EGFR phosphorylation inhibitory activity assay

The ability of the prepared derivatives to inhibit EGFR kinase activity was assessed using ADP-Glo™ Kinase Assay kit (Promega) according to the manufacturer's instructions. Briefly, the assays were carried out in 96-well plates in a final volume of 20 μL containing 1 × reaction buffer, 50 μM DTT, 2 mM $MnCl_2$, 5 μg substrate, 10 μM ATP, and 30 ng of wild-type human recombinant EGFR expressed in sf9 insect cells. The enzyme incubated with 1 μM concentrations of each derivative as well as the standard gefitinib for 10 min at room temperature prior to the kinase reaction. Kinase reactions were initiated by adding ATP and substrate and incubated for 25 min at room temperature. Then, 20 μL ADP-Glo™ Reagent (promega) was added to stop the kinase reaction and the reaction mixture was incubated for 50 min. After adding the kinase detection reagent, the EGFR activity was determined by measuring the luminescence of the reaction mixture. Data are presented as the means of three independent experiments.

Results

Convergent synthesis was adopted for preparation of the targeted alkylphosphocholine-gefitinib conjugates (**4**). First, gefitinib core tethered with linkers were synthesized as shown in Scheme 1. The easily prepared 4-chloroquinazoline derivative **5** (Schwan et al. 2014) upon aromatic nucleophilic substitution with 3-chloro-4-

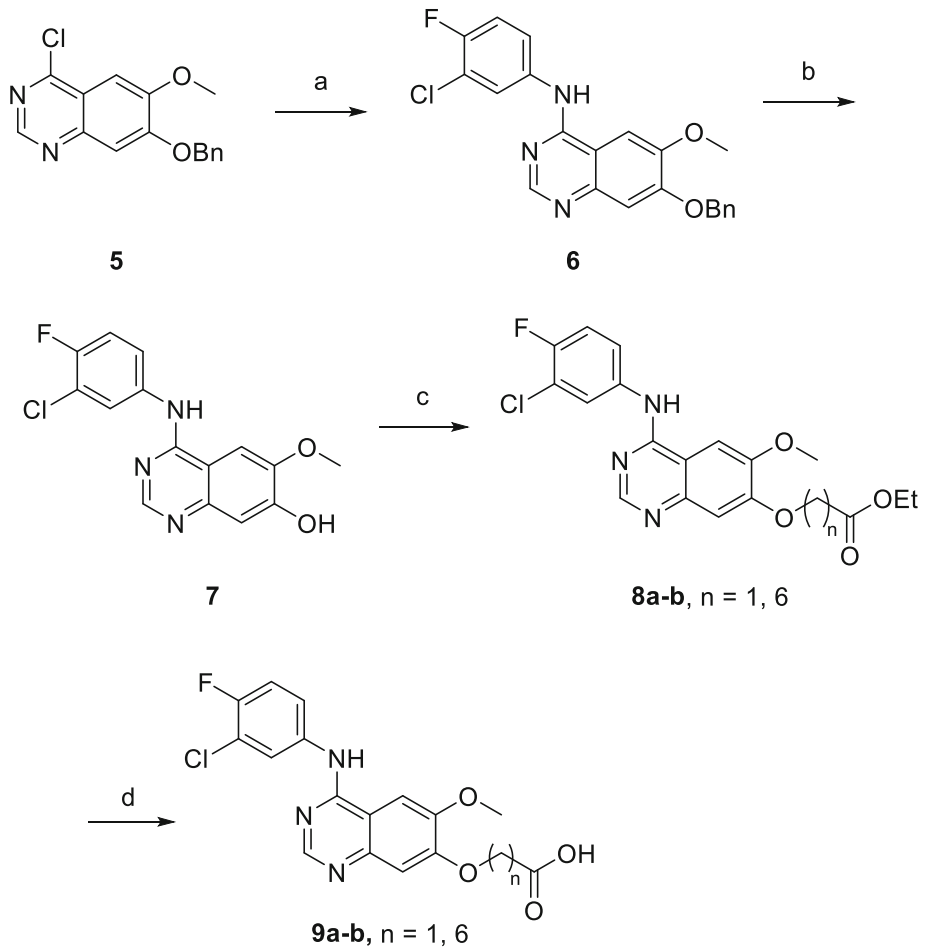

Scheme 1 Reagents and conditions: **a** 3-chloro-4-fluoroaniline, reflux, 96%; **b** TFA, reflux, 98%; **c** K_2CO_3, ethyl bromoalkanoate, 62 °C, 89 ~ 71%; **d** LiOH, rt, 91 ~ 92%

fluoroaniline afforded the core of gefitinib **6** as 7-benzyloxy protected derivative. Deprotection with trifluoroacetic acid yielded the hydroxyl derivative **7** for tethering with linkers. Tethers were attached via alkylation with corresponding ethyl bromoalkanoates to afford derivatives **8**. Hydrolysis with lithium hydroxide provided carboxylic acids **9** ready for coupling with alkylphosphocholine derivatives.

As shown in Scheme 2A, the benzyloxy derivatives **10** (Raghavan and Krishnaiah 2010; Verma et al. 2016) were converted to benzyloxyalkylphosphocholines **11** via reaction with 2-chloro-1,3,2-dioxaphospholane-2-oxide followed by opening of the dioxaphospholane ring with anhydrous trimethylamine. Hydrogenation affords the unprotected hydroxyl derivatives **12** ready for conjugation with the prepared carboxylic acids **9**. Finally, as illustrated in Scheme 2B, DCC-promoted coupling of carboxylic acids **9** and hydroxyl derivatives **12** yielded the desired alkylphosphocholine-gefitinib conjugates (**4**).

Gefitinib is primarily used for lung cancer treatment. However, it has been also considered as a single or in combination treatment for breast cancer (Gutteridge et al. 2010; Girgert et al. 2017; Wu et al. 2017), liver cancer (Höpfner et al. 2004; Desbois-Mouthon et al. 2006; Shao et al. 2016) and skin cancer (Godugu et al. 2016). Accordingly, for the evaluation of the antiproliferative activity of the prepared gefitinib-APC conjugates, four cell lines were employed representing lung, breast, liver and skin cancers (non-small-cell lung adenocarcinoma cells line A-549; breast adenocarcinoma cell line MCF-7, liver hepatocellular carcinoma cell line HepG2, and epidermoid squamous carcinoma cell line A-431). As shown in Table 1, gefitinib shows high micromolar IC_{50} values against these cell lines. Three reference standard anticancer agents were used. Two of them (gefitinib and erlotinib) are EGFR kinase inhibitors while the third (miltefosine) is a standard alkylphosphocholine derivative. With regard to the length of the linker's chain, two series of compounds were prepared and evaluated. The results are presented in Table 1.

As alkylphosphocholines are known to inhibit Akt phosphorylation (Alam et al. 2012, 2013), the ability of the

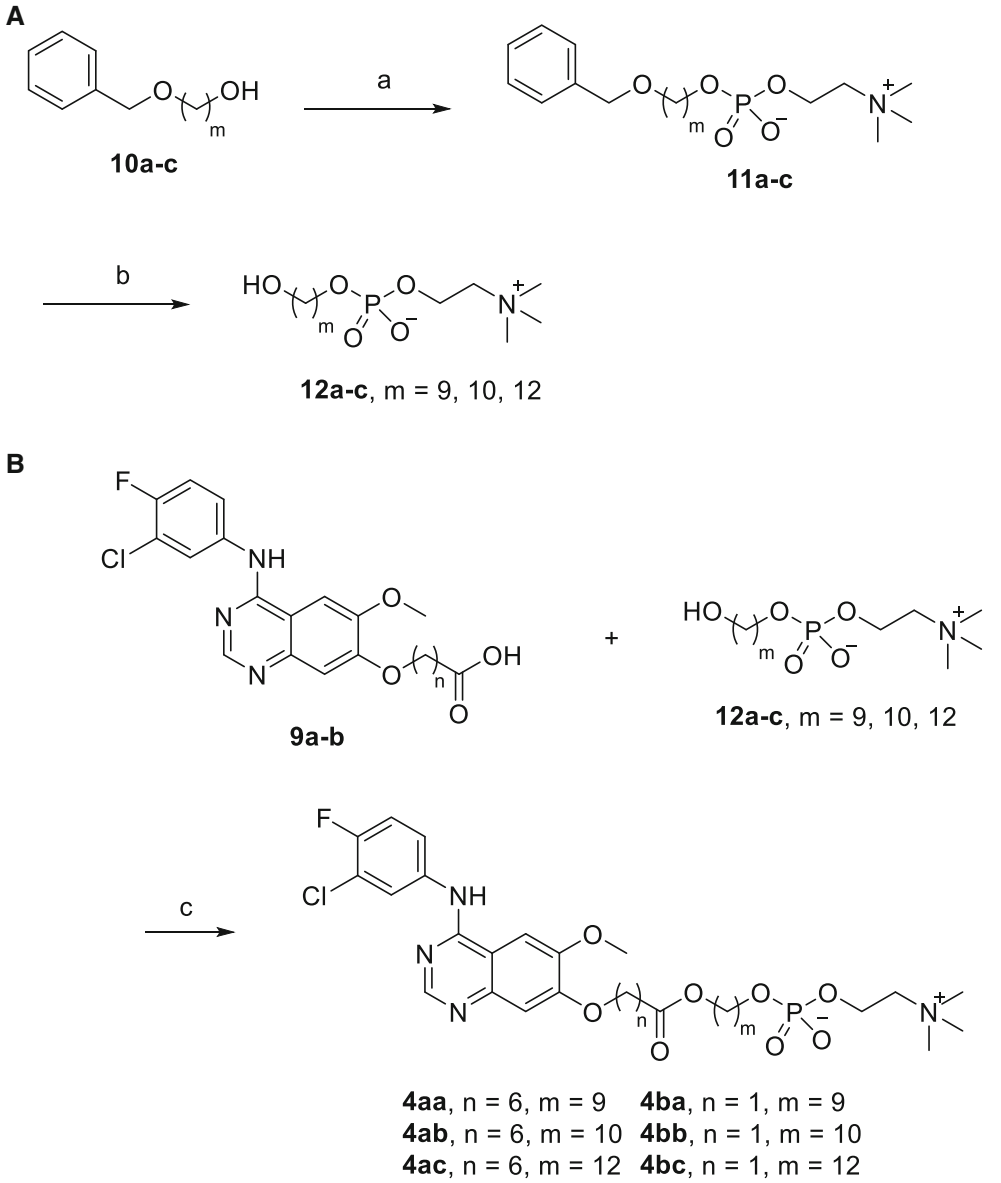

Scheme 2 Reagents and conditions: **a** (i) 2-Chloro-1,3,2-dioxaphospholane-2-oxide, TEA, rt; (ii) TMA, 65 °C, 88 ~ 53% over 2 steps; **b** H_2, Pd/C, MeOH, rt, 96 ~ 92%; **c** DCC, DMAP, $CHCl_3$, reflux, 88 ~ 50%

prepared gefitinib-APCs conjugates **4** to inhibit Akt phosphorylation were measured by cell based assay using miltefosine as a reference standard. Thus, A549 cells pretreated with 20 μM concentration of each compound or the standard miltefosine were stimulated to undergo Akt phosphorylation for 30 min after which cells were lysed and phosphorylated Akt was assayed in the lysate to calculate the percent inhibition of Akt phosphorylation. The results are shown in Table 1.

Next to the assay of the ability of the prepared conjugates **4** to inhibit phosphorylation of Akt, determination of the inhibitory activity EGFR kinase reaction was addressed. Using ADP-Glo™ kinase assay kit, the remaining EGFR activity after treatment with 1 μM concentrations of the most active conjugates series (**4aa**, **4ab** and **4ac**) and gefitinib was determined. The results are in Table 1.

Discussion

The results, as indicated in Table 1, revealed that the longer linker's alkyl chain series (m = 6) possesses higher activity than the shorter linker's alkyl chain series (m = 1). Among the used four cell lines, breast cancer cell line MCF-7 showed the highest sensitivity to the prepared

Table 1 Cytotoxicity against human cancer cell lines, inhibition of Akt Phosphorylation and EGFR kinase reaction of gefitinib-APC conjugates **4**

Compd.	MCF-7		A431		HepG2		A549		% Akt Phos. Inhib.[c]	% EGFR Inhib.[d]
	% GI[a]	IC_{50}[b]	% GI	IC_{50}	% GI	IC_{50}	% GI	IC_{50}		
Gefitinib	89.2	40.1	75.8	36.1	92.9	26.7	89.2	40.7	–	98.7 ± 0.8
Erlotinib	33.2	–	47.0	–	36.7	–	48.2	–	–	–
Miltefosine	31.2	–	35.3	–	31.2	–	36.6	–	87.0 ± 4.1	–
4aa	53.6	–	48.6	–	29.1	–	29.5	–	26.6 ± 7.5	87.4 ± 0.4
4ab	54.4	–	19.8	–	36.8	–	31.7	–	28.1 ± 1.8	75.5 ± 2.6
4ac	45.8	–	46.4	–	19.3	–	13.4	–	31.3 ± 5.4	70.0 ± 2.0
4ba	6.2	–	15.9	–	6.9	–	–	–	8.3 ± 3.6	–
4bb	1.6	–	17.5	–	10.9	–	14.2	–	8.4 ± 3.6	–
4bc	14.9	–	12.1	–	–	–	–	–	3.1 ± 2.3	–

[a]% Growth inhibition at 100 μM

[b]Micromolar concentration that inhibits growth by 50%

[c]Percent inhibition of Akt phosphorylation in A549 cells at 20 μM

[d]Percent inhibition of EGFR kinase at 1 μM

conjugates. The measured growth inhibition percent for derivatives **4aa** and **4ab** was around 54% while it was lower ($\approx$ 46%) for derivative **4ac**. Despite these values for inhibition percent are lower than that of gefitinib, they are still better than those for erlotinib and miltefosine. The response of skin cancer cell line A431 to derivatives **4aa** and **4ac** (around 49 and 46% respectively) was not far from that response for erlotinib (47%), but significantly higher than that of miltefosine (35%) and lower than that of gefitinib ($\approx$ 76%). In contrast, the response for derivative **4ab** was weak in inducing inhibition of the proliferation of A431 cell line. However, the response of liver cancer cell line HepG2 to compound **4ab** was almost similar to erlotinib ($\approx$ 37%) and higher than that for miltefosine but lower than gefitinib. While the response of HepG2 cell line to derivative **4ac** was lower than all of responses to gefitinib, erlotinib and miltefosine, it showed response to **4aa** near to miltefosine. The response of the last used cell line which represent lung cancer A549 to derivatives **4aa**, **4ab** and **4ac** was weaker than responses to gefitinib, erlotinib and miltefosine. Nevertheless, responses to derivatives **4aa** and **4ab** were significant and they were lower by 5 $\sim$ 7 percent units relative to the response to miltefosine. Collectively, these results show that the profiles of derivatives **4aa**, **4ab** and **4ac** over the tested cell lines are discrete from the profile of gefitinib. They are more skewed toward the profile of miltefosine, although they are still distinct.

On the other side, the responses to derivatives **4ba**, **4bb**, and **4bc** with the short linker were very weak over the used four cell lines. The best measured response among this series was 17.5% growth inhibition by derivative **4bb** against A431 cell line. Responses to this derivative by A549, HepG2 and MCF-7 were as low as 14.2, 10.9 and 1.6% growth inhibition respectively. In spite that derivative **4bc** did not elicit inhibition of growth of two cell lines (HepG2 and A549), it showed the best percent of growth inhibition ($\approx$ 15%) among the short linker series against MCF-7 cell line. It was also the least active among this series against A431 cell line ($\approx$ 12%). Also, derivative **4ba** did not show any inhibition of A549 cell line and showed weak inhibitions against MCF-7, HepG2 and A431 (around 6, 7 and 16% respectively). These results show that the longer linker chain length are in favor of more antiproliferative effect.

The assay of inhibition of Akt phosphorylation, as indicated in Table 1, revealed that the standard miltefosine effectively induced 87% inhibition of Akt phosphorylation. Paradoxically, the prepared conjugates **4** were not effective inhibitors of Akt phosphorylation. The maximum inhibitory activity for Akt phosphorylation was 31.3% for derivative **4ac**. Even with the measured low inhibitions, the results revealed that conjugates **4aa**, **4ab** and **4ac** possessing the longer linker induce higher Akt inhibition values than the corresponding conjugates **4ba**, **4bb** and **4bc** with the shorter linker. This difference in Akt phosphorylation inhibition is proportional to the observed difference in the antiproliferative activity of both series. This might indicates that the length of the linker is crucial for the elicited inhibition of Akt phosphorylation. Development of conjugates with better inhibitory activity might results in more effective antiproliferative activity.

As revealed from the obtained results (Table 1), the standard gefitinib inhibited almost all of the EGFR activity (98.7%). The tested conjugates at the used concentration produced high inhibitions of EGFR kinase reaction, albeit, incomplete inhibitions was achieved. The highest achieved

inhibition value induced by conjugates was for the **4aa** with the smallest alkyl chain (87.4%). The EGFR inhibitory activity decreases with increasing the chain length. This is clear from the measured values for **4ab** with the longer chain length (75.5%) and for **4ac** with the longest chain length (70%). This is in inverse relation to the revealed behavior of inhibition of Akt phosphorylation which increases with increasing chain length (26.6, 28.1 and 31.3% for **4aa**, **4ab** and **4ac** respectively). These results may indicate a needed careful balancing between the inhibition of both of Akt phosphorylation and EGFR kinase reaction.

In summary, two series of novel conjugates of alkylphosphocholines and gefitinib were designed and prepared as multitarget antiproliferative agents. While the conjugates series with short chain length linker elicited weak antiproliferative efficacy, the conjugates series with the longer chain length linker possessed efficacy comparable to erlotinib and miltefosine, however, weaker than gefitinib. Despite that, the performed study provides insights on the balance between the inhibitions of the Akt phosphorylation and EGFR kinase reaction in the studied conjugates. This strategy might offer opportunities for preparation of more effective chemical entities by implementing the gained lessons from this study to achieve a better design of multitarget antiproliferative agents.

Acknowledgements This research was supported by the "Basic Science Research Program" through the "National Research Foundation of Korea (NRF)" funded by MEST, Republic of Korea (#2012-006431).

Compliance with ethical standards

Conflict of interest The authors declare that they have no conflict of interest.

References

Alam MM, Joh E-H, Kim Y, Oh YI, Hong J, Kim B, Kim D-H, Lee YS (2012) Synthesis and biological evaluation of cyclopentane-linked alkyl phosphocholines as potential anticancer agents that act by inhibiting Akt phosphorylation. Eur J Med Chem 47:485–492

Alam MM, Joh E-H, Park H, Kim B, Kim D-H, Lee YS (2013) Synthesis, characterization and Akt phosphorylation inhibitory activity of cyclopentanecarboxylate-substituted alkylphosphocholines. Biorgan Med Chem 21:2018–2024

Beloribi-Djefaflia S, Vasseur S, Guillaumond F (2016) Lipid metabolic reprogramming in cancer cells. Oncogenesis 5:e189

Block M, Grundker C, Fister S, Kubin J, Wilkens L, Mueller MD, Hemmerlein B, Emons G, Gunthert AR (2012) Inhibition of the AKT/mTOR and erbB pathways by gefitinib, perifosine and analogs of gonadotropin-releasing hormone I and II to overcome tamoxifen resistance in breast cancer cells. Int J Oncol 41:1845–1854

Calay D, Vind-Kezunovic D, Frankart A, Lambert S, Poumay Y, Gniadecki R (2010) Inhibition of Akt signaling by exclusion from lipid rafts in normal and transformed epidermal keratinocytes. J Invest Dermatol 130:1136–1145

Clive S, Gardiner J, Leonard RC (1999) Miltefosine as a topical treatment for cutaneous metastases in breast carcinoma. Cancer Chemother Pharmacol 44(Suppl):S29–S30

Danker K, Reutter W, Semini G (2010) Glycosidated phospholipids: uncoupling of signalling pathways at the plasma membrane. Br J Pharmacol 160:36–47

Desbois-Mouthon C, Cacheux W, Blivet-Van Eggelpoel MJ, Barbu V, Fartoux L, Poupon R, Housset C, Rosmorduc O (2006) Impact of IGF-1R/EGFR cross-talks on hepatoma cell sensitivity to gefitinib. Int J Cancer 119:2557–2566

Dragowska WH, Weppler SA, Qadir MA, Wong LY, Franssen Y, Baker JH, Kapanen AI, Kierkels GJ, Masin D, Minchinton AI, Gelmon KA, Bally MB (2011) The combination of gefitinib and RAD001 inhibits growth of HER2 overexpressing breast cancer cells and tumors irrespective of trastuzumab sensitivity. BMC Cancer 11:420

Faustino M (2014) Editorial (thematic issue: antitumor alkylphospholipid analogs: a promising and growing family of synthetic cell membrane-targeting molecules for cancer treatment). Anticancer Agents Med Chem 14:495–498

Fedida-Metula S, Elhyany S, Tsory S, Segal S, Hershfinkel M, Sekler I, Fishman D (2008) Targeting lipid rafts inhibits protein kinase B by disrupting calcium homeostasis and attenuates malignant properties of melanoma cells. Carcinogenesis 29:1546–1554

Fielding CJ, Fielding PE (2004) Membrane cholesterol and the regulation of signal transduction. Biochem Soc Trans 32:65–69

Girgert R, Emons G, Grundker C (2017) 17beta-estradiol-induced growth of triple-negative breast cancer cells is prevented by the reduction of GPER expression after treatment with gefitinib. Oncol Rep 37:1212–1218

Godugu C, Doddapaneni R, Patel AR, Singh R, Mercer R, Singh M (2016) Novel gefitinib formulation with improved oral bioavailability in treatment of A431 skin carcinoma. Pharm Res 33:137–154

Gomez-Serranillos IR, Minones J Jr, Dynarowicz-latka P, Miniones J, Iribarnegaray E (2004) Miltefosine–cholesterol interactions: a monolayer study. Langmuir 20:928–933

Gutteridge E, Agrawal A, Nicholson R, Leung Cheung K, Robertson J, Gee J (2010) The effects of gefitinib in tamoxifen-resistant and hormone-insensitive breast cancer: a phase II study. Int J Cancer 126:1806–1816

Höpfner M, Sutter AP, Huether A, Schuppan D, Zeitz M, Scherubl H (2004) Targeting the epidermal growth factor receptor by gefitinib for treatment of hepatocellular carcinoma. J Hepatol 41:1008–1016

Kazandjian D, Blumenthal GM, Yuan W, He K, Keegan P, Pazdur R (2016) FDA approval of gefitinib for the treatment of patients with Metastatic EGFR mutation-positive non-small cell lung cancer. Clin Cancer Res 22:1307–1312

Kostadinova A, Topouzova-Hristova T, Momchilova A, Tzoneva R, Berger MR (2015) Antitumor lipids—structure, functions, and medical applications. In: Rossen D (ed) Advances in protein chemistry and structural biology. Academic Press, pp 27–66

Li H, Zhou S, Li X, Wang D, Wang Y, Zhou C, Schmid-Bindert G (2013) Gefitinib-resistance is related to BIM expression in non-small cell lung cancer cell lines. Cancer Biother Radiopharm 28:115–123

Malta de Sá M, Sresht V, Rangel-Yagui CO, Blankschtein D (2015) Understanding miltefosine–membrane interactions using molecular dynamics simulations. Langmuir 31:4503–4512

Murray M, Hraiki A, Bebawy M, Pazderka C, Rawling T (2015) Anti-tumor activities of lipids and lipid analogues and their development as potential anticancer drugs. Pharmacol Ther 150:109–128

Pachioni Jde A, Magalhaes JG, Lima EJ, Bueno Lde M, Barbosa JF, de Sa MM, Rangel-Yagui CO (2013) Alkylphospholipids—a promising class of chemotherapeutic agents with a broad pharmacological spectrum. J Pharm Pharm Sci 16:742–759

Pike LJ (2003) Lipid rafts: bringing order to chaos. J Lipid Res 44:655–667

Raghavan S, Krishnaiah V (2010) An efficient stereoselective synthesis of penaresidin A from (E)-2-protected amino-3,4-unsaturated sulfoxide. J Org Chem 75:748–761

Reis-Sobreiro M, Roué G, Moros A, Gajate C, de la Iglesia-Vicente J, Colomer D, Mollinedo F (2013) Lipid raft-mediated Akt signaling as a therapeutic target in mantle cell lymphoma. Blood Cancer J 3:e118

Schwan G, Barbar Asskar G, Höfgen N, Kubicova L, Funke U, Egerland U, Zahn M, Nieber K, Scheunemann M, Sträter N, Brust P, Briel D (2014) Fluorine-containing 6,7-dialkoxybiaryl-based inhibitors for phosphodiesterase 10 A: synthesis and in vitro evaluation of inhibitory potency, selectivity, and metabolism. ChemMedChem 9:1476–1487

Shao J, Xu Z, Peng X, Chen M, Zhu Y, Xu L, Zhu H, Yang B, Luo P, He Q (2016) Gefitinib synergizes with irinotecan to suppress hepatocellular carcinoma via antagonizing Rad51-Mediated DNA-repair. PLoS ONE 11:e0146968

Simons K, Toomre D (2000) Lipid rafts and signal transduction. Nat Rev Mol Cell Biol 1:31–39

van Blitterswijk WJ, Verheij M (2013) Anticancer mechanisms and clinical application of alkylphospholipids. BBA Mol Cell Biol Lipids 1831:663–674

Verma YK, Reddy BS, Pawar MS, Bhunia D, Sampath Kumar HM (2016) Design, synthesis, and immunological evaluation of benzyloxyalkyl-substituted 1,2,3-triazolyl α-GalCer analogues. ACS Med Chem Lett 7:172–176

Weichert JP, Clark PA, Kandela IK, Vaccaro AM, Clarke W, Longino MA, Pinchuk AN, Farhoud M, Swanson KI, Floberg JM, Grudzinski J, Titz B, Traynor AM, Chen H-E, Hall LT, Pazoles CJ, Pickhardt PJ, Kuo JS (2014) Alkylphosphocholine analogs for broad-spectrum cancer imaging and therapy. Sci Transl Med 6(240):275

Wu Y, Zhang D, Wu B, Quan Y, Liu D, Li Y, Zhang X (2017) Synergistic activity of an antimetabolite drug and tyrosine kinase inhibitors against breast cancer cells. Chem Pharm Bull. doi:10.1248/cpb.c17-00261

Zhuang L, Kim J, Adam RM, Solomon KR, Freeman MR (2005) Cholesterol targeting alters lipid raft composition and cell survival in prostate cancer cells and xenografts. J Clin Invest 115:959–968